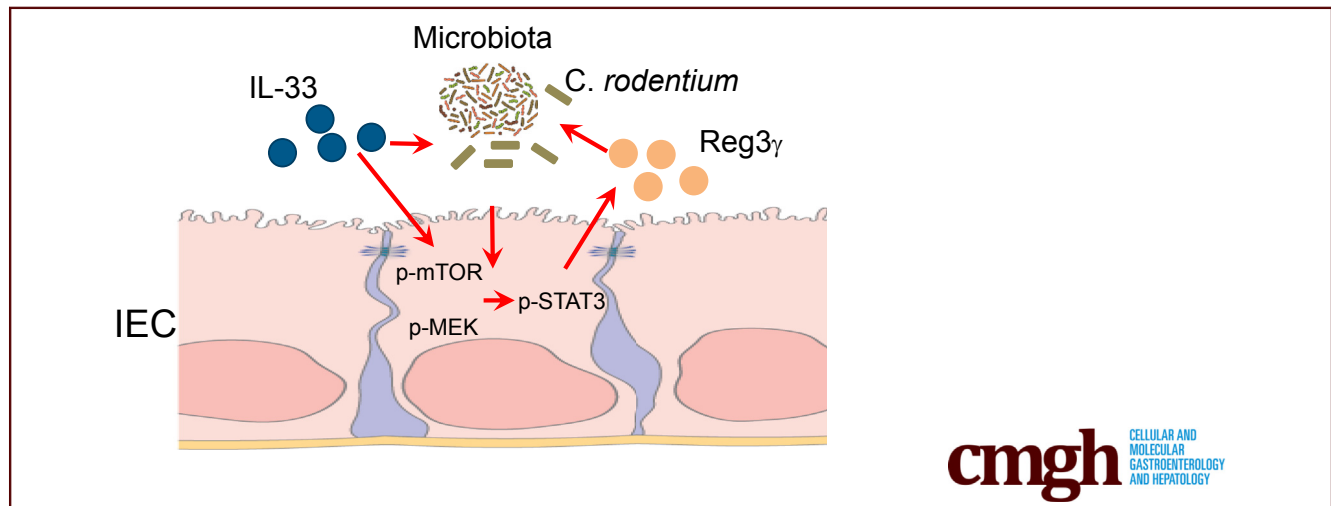


ORIGINAL RESEARCH

Interleukin-33 Promotes REG3 γ Expression in Intestinal Epithelial Cells and Regulates Gut Microbiota

Yi Xiao,^{1,2,*} Xiangsheng Huang,^{1,*} Ye Zhao,¹ Feidi Chen,³ Mingming Sun,^{1,4} Wenjing Yang,^{1,4} Liang Chen,^{1,4} Suxia Yao,¹ Alex Peniche,⁵ Sara M. Dann,⁵ Jiaren Sun,¹ George Golovko,⁶ Yuriy Fofanov,⁶ Yinglei Miao,⁷ Zhanju Liu,⁴ Daiwen Chen,² and Yingzi Cong^{1,3}

¹Department of Microbiology and Immunology, University of Texas Medical Branch, Galveston, Texas; ²Key Laboratory of Animal Disease-Resistance Nutrition, Animal Nutrition Institute, Sichuan Agricultural University, Yaan, Sichuan, China; ³Department of Pathology, University of Texas Medical Branch, Galveston, Texas; ⁴Department of Gastroenterology, The Shanghai Tenth People's Hospital, Tongji University, Shanghai, China; ⁵Department of Internal Medicine, University of Texas Medical Branch, Galveston, Texas; ⁶Department of Pharmacology and Toxicology, University of Texas Medical Branch, Galveston, Texas; ⁷Department of Gastroenterology, The First Affiliated Hospital of Kunming Medical University, Kunming, China



SUMMARY

Interleukin-33 promotes intestinal epithelial cells production of the antimicrobial peptide REG3 γ , which is mediated by mTOR, STAT3, and ERK1/2. Furthermore, interleukin-33 controls gut microbiota, and enhances the capability of intestinal epithelial cells to limit bacteria survival, possibly through induction of REG3 γ .

BACKGROUND & AIMS: Regenerating islet-derived protein (REG3 γ), an antimicrobial peptide, typically expressed by intestinal epithelial cells (IEC), plays crucial roles in intestinal homeostasis and controlling gut microbiota. However, the mechanisms that regulate IEC expression of REG3 γ are still largely unclear. In this study, we investigated whether and how interleukin (IL) 33, an alarmin produced by IEC in response to injury, regulates REG3 γ expression in IEC, thus contributing to intestinal homeostasis.

METHODS: IEC were isolated from wild-type and IL33^{-/-} mice to determine expression of REG3 γ and other antimicrobial peptides by quantitative real-time polymerase chain reaction and Western blot. IEC cell lines were used for mechanistic studies. 16S rRNA pyrosequencing analysis was used for measuring gut microbiota. *Citrobacter rodentium* was used for enteric infections.

RESULTS: The expression of REG3 γ , but not β -defensins, in IECs of IL33^{-/-} mice was significantly lower than wild-type mice. IL33 treatment induced IEC expression of REG3 γ in both mice and human cell lines. Mechanistically, IL33 activated STAT3, mTOR, and ERK1/2 in IEC. Inhibition of these pathways abrogated IL33-induction of REG3 γ . IL33^{-/-} mice demonstrated higher bacteria loads and altered microbiota composition. IL33 did not directly inhibit bacterial growth, but promoted wild-type, not REG3 γ KO, IECs to kill bacteria *in vitro*. Consistently, *C. rodentium* infection induced IEC IL33 expression, and IL33^{-/-} mice demonstrated an impaired bacterial clearance with *C. rodentium* infection.

CONCLUSIONS: Our study demonstrated that IL33, which is produced by IEC in response to injury and inflammatory stimulation, in turn promotes IEC expression of REG3 γ , and controls the gut microbiota of the host. (*Cell Mol Gastroenterol Hepatol* 2019;8:21–36; <https://doi.org/10.1016/j.jcmgh.2019.02.006>)

Keywords: IEC; IL33; REG3 γ ; Microbiota.

The intestinal epithelium is in direct contact with the external environment that contains tens of trillions of microorganisms. Shaped by coevolution with the microbiota, the host has evolved unique regulatory mechanisms to maintain a homeostatic balance between tolerance and immunity to the microbiota.¹ The epithelium, comprised of single layer of predominately intestinal epithelial cells (IEC), plays a vital role in the crosstalk between immune cells and the microbiota by forming a physical barrier between the lumen and the submucosa. To protect the barrier, IEC and Paneth cells secrete numerous substances and molecules, such as antimicrobial peptides (AMPs).^{2,3} There are several distinct protein families of AMPs produced in the intestine, including defensins, cathelicidins, and C-type lectins, such as the regenerating islet-derived protein (REG) family.⁴ Among REG3 lectins, REG3 γ is the most widely expressed AMP in the small intestine of mice and humans, and is known for its selective activity toward bacteria,^{4,5} and for its expression in the large intestine during inflammation or microbial infection.⁶ Although both the microbiota and interleukin (IL) 22 have been shown to stimulate IEC expression of certain AMPs, including REG3 γ , the mechanisms that regulate IEC AMP production are still not completely understood.

As a member of the IL1 cytokine family, IL33 (also known as IL1F11) is abundantly produced by IEC, especially during inflammation or injury,^{7,8} which classifies IL33 as an alarmin (alarm signal). However, the role of IL33 in intestinal homeostasis still remains controversial. This is because protective and pathologic roles for IL33 have been demonstrated in murine models of acute colitis.^{9–14} IL33 is suggested to have proinflammatory effects by activating several immune cells including T-helper cell type 2 cells and basophils.^{10,12} However, it has also been shown that IL33 inhibits experimental colitis in mice through promoting T-helper cell type 2/Foxp3⁺ regulatory T-cell responses.⁹ Thus, the mechanisms involved in the crosstalk between IL33 and the intestinal immune responses are still largely unclear. Moreover, as yet, the potential roles of IL33 in regulating AMPs and in controlling gut microbiota symbiosis have not been well studied.

In this report, we demonstrate a significant reduction of REG3 γ expression in IEC of IL33^{-/-} mice compared with the wild-type (WT) mice, suggesting that IL33 is crucial for REG3 γ expression by IEC. IL33 treatment promoted REG3 γ production by both human and murine IEC, and mouse intestinal enteroids. IL33^{-/-} mice demonstrated an increased number in gut microbiota and altered composition. On oral infection, IL33^{-/-} mice allowed more *Citrobacter rodentium* growth in the intestines compared with WT mice. Furthermore, IL33-treated WT, but not

REG3 γ ^{-/-}, IEC inhibited bacterial growth. Our study, thus, demonstrated a novel role of IL33 in regulation of gut microbiota through the induction of IEC REG3 γ .

Results

REG3 γ Production in IEC Was Impaired in IL33^{-/-} Mice

To investigate whether IL33 regulates IEC production of AMPs, we isolated IEC from the intestines of WT and IL33^{-/-} mice and assessed the expression of REG3 γ and other AMPs by quantitative real-time polymerase chain reaction (qRT-PCR) for gene expression and Western blot analysis for protein production. Our results showed that REG3 γ production was significantly lower at both mRNA level (Figure 1A) and protein level (Figure 1B) in IEC of IL33^{-/-} mice compared with WT mice, indicating IL33 is 1 of the important factors contributing to the induction of REG3 γ in IEC *in vivo*. However, deficiency of IL33 did not affect IEC expression of defensin-1, -2, -3, and -4, because the expression of those defensins showed no difference in IEC from WT versus IL33^{-/-} mice (Figure 1C).

It has been reported that IL33 is constitutively expressed by endothelial cells in blood vessels and epithelial cells at various barrier tissues under steady conditions.^{8,15} To determine whether IEC expresses IL33 under steady conditions, we isolated IEC from WT mice. Because it has been shown that IL33 expression in IEC is increased on inflammation, we also isolated IEC from inflamed intestines of the mice suffered from colitis on Dextran sulfate sodium (DSS) insults to serve as the positive control. We then determined IL33 production in IEC by qRT-PCR for gene expression, enzyme-linked immunosorbent assay, and Western blot for protein levels. IEC produced IL33 at a low level under steady conditions, which was increased in IEC of the mice with colitis (Figure 1D–F).

IL33 Promoted Expression of REG3 γ in Both Mouse and Human IEC In Vitro

To determine whether IL33 directly promotes IEC expression of REG3 γ , we treated MSIE, an immortalized epithelial cell line established from the intestines of normal mice,¹⁶ with IL33 for 12 hours, and then measured the expression of REG3 γ and β -defensins. As shown in Figure 2A, IL33 treatment significantly induced the expression of REG3 γ , but not β -defensins-1, -3, and -4, in a dose-dependent manner. We also determined the kinetics of REG3 γ expression induced by IL33. MSIE were treated with

*These authors contributed equally to this work.

Abbreviations used in this paper: AMP, antimicrobial peptides; IEC, intestinal epithelial cells; IL, interleukin; NF, nuclear factor; PBS, phosphate-buffered saline; qRT-PCR, quantitative real-time polymerase chain reaction; REG, regenerating islet-derived protein; siRNAs, short interfering RNAs; WT, wild-type.



Most current article

© 2019 The Authors. Published by Elsevier Inc. on behalf of the AGA Institute. This is an open access article under the CC BY-NC-ND license (<http://creativecommons.org/licenses/by-nc-nd/4.0/>).

2352-345X

<https://doi.org/10.1016/j.jcmgh.2019.02.006>

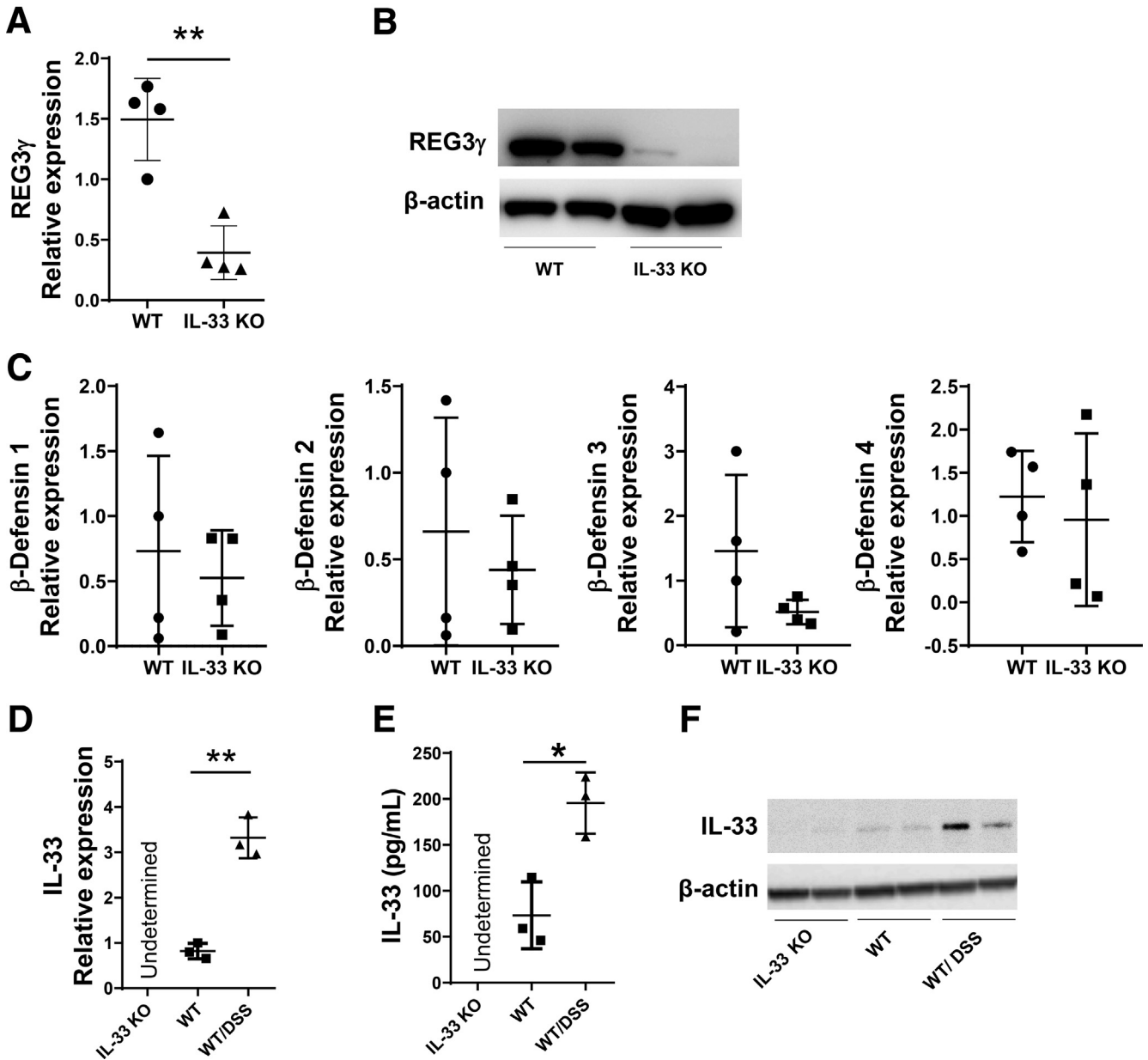


Figure 1. REG3 γ expression in IEC was impaired in IL33 $^{-/-}$ mice. (A–C) IECs were isolated from small intestines of WT and IL33 $^{-/-}$ mice ($n = 4$ /group). The expression of REG3 γ was determined by qRT-PCR and normalized against glyceraldehyde-3-phosphate dehydrogenase (phosphorylating) (GAPDH) (A), and by Western blot, with β -actin as the loading control (B). The expression of β -defensin-1, -2, -3, and -4 was determined by qRT-PCR and normalized against GAPDH (C). (D–F) WT mice ($n = 3$ /group) were fed with 1.65% (wt/vol) DSS in drinking water for 7 days and water alone for additional 3 days to induce colitis. IL33 expression in IEC of IL33 $^{-/-}$ mice, WT mice, and colitic WT mice with Dextran sulfate sodium (DSS) was measured by qRT-PCR and normalized against GAPDH (D), enzyme-linked immunosorbent assay (E), and Western blot (F). Significance was calculated using an unpaired Student t test. * $P < .05$, ** $P < .01$. Data are represented as means \pm standard deviation. One representative of 3 experiments with similar results.

IL33, and REG3 γ expression was measured at different time points from 1 hour to 24 hours. REG3 γ in MSIE cells was increased starting from 6 hours after IL33 treatment, reaching the plateau at 12 hours, and fading gradually thereafter (Figure 2B). To further confirm the results, we treated WT enteroids with IL33.

As shown in Figure 2C, IL33 promoted enteroid expression of REG3 γ . To rule out off target effect of IL33, we

generated ST2, receptor of IL33, knockout (ST2 KO) MSIE cells by CRISPR, and then treated WT and ST2 KO cells with IL33. Notably, baseline of REG3 γ expression in ST2 KO MSIE cells was decreased compared with WT MSIE cells. Although IL33 induced WT MSIE cell expression of REG3 γ , it did not promote ST2 KO MSIE cell REG3 γ expression (Figure 2D). We also investigated whether IL33 stimulated production of itself in IEC as a positive loop to promote REG3 γ . We

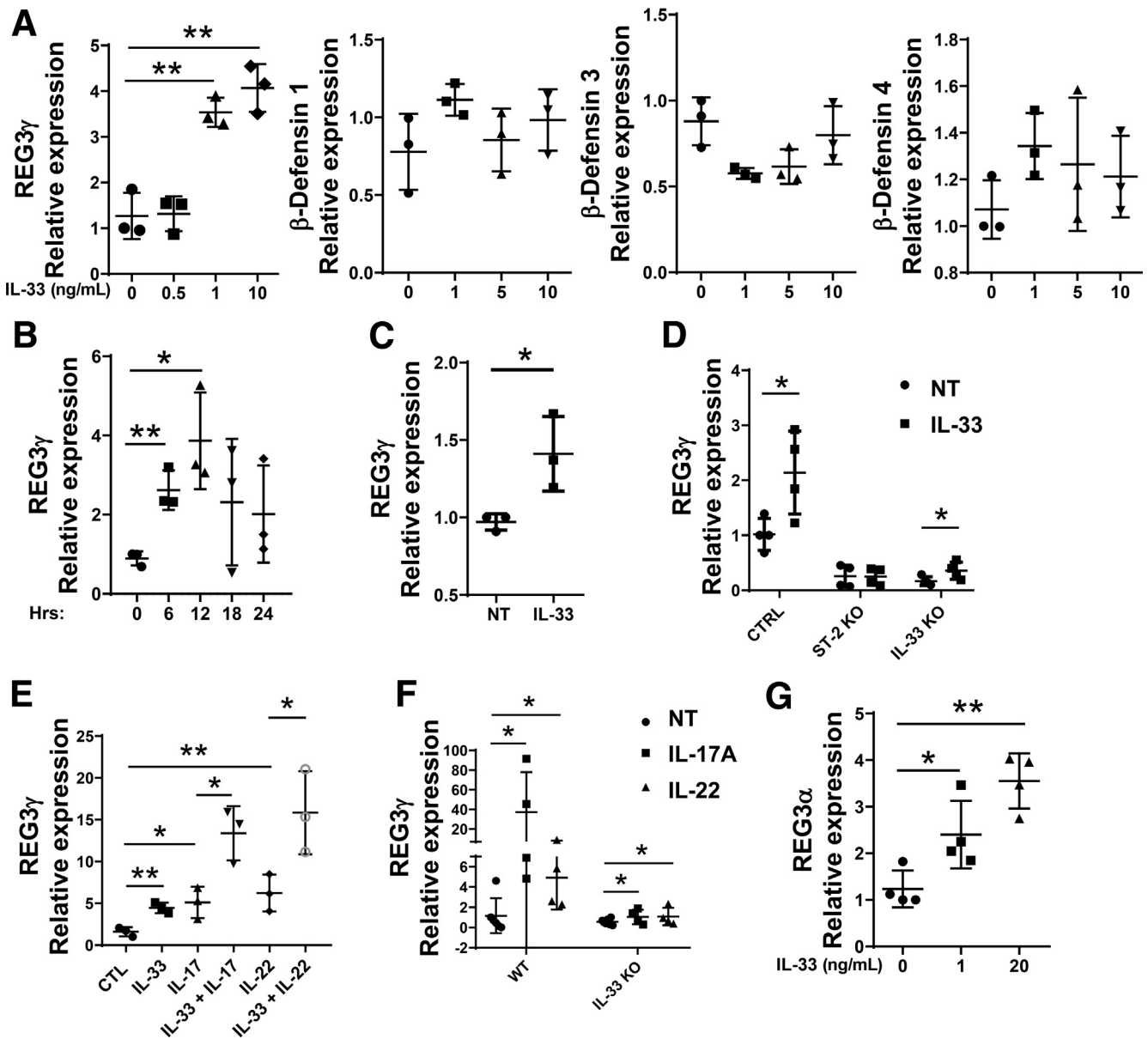


Figure 2. IL33 promotes expression of REG3 γ in both murine and human IEC. (A) MSIE cells ($n = 3$ wells/group) were treated with a series of doses of IL33 for 12 hours. The expression of REG3 γ , β -defensin-1, -3, and -4 was determined by qRT-PCR, and normalized against glyceraldehyde-3-phosphate dehydrogenase (phosphorylating) (GAPDH). (B) MSIE cells ($n = 3$ wells/group) were treated with 10 ng/mL of IL33. The expression of REG3 γ was determined at different time points from 0 hours to 24 hours by qRT-PCR and normalized against GAPDH. (C) WT enteroids ($n = 3$ wells/group) were treated with IL33 (20 ng/mL) for 48 hours, and REG3 γ expression was determined by qRT-PCR and normalized against GAPDH. (D) ST2 knockout (ST2 KO) and IL33 knockout (IL33 KO) MSIE cells ($n = 4$ wells/group), generated by CRISPR, were treated with 10 ng/mL of IL33 together with WT MSIE cells. The expression of REG3 γ was determined by qRT-PCR and normalized against GAPDH. (E) MSIE cells ($n = 3$ wells/group) were treated with 10 ng/mL of IL17 or IL22 in the presence or absence of 10 ng/mL of IL33 for 12 hours. The expression of REG3 γ was determined by qRT-PCR and normalized against GAPDH. (F) WT ($n = 4$) and IL33 $^{-/-}$ mice ($n = 4$) were administered intraperitoneally with IL17 (1 μ g/mouse) daily or IL22 (2 μ g/mouse) every other day for 10 days. The IEC expression of REG3 γ was determined by qRT-PCR and normalized against GAPDH. (G) Human HT-29 cells ($n = 4$ wells/group) were treated with a series of doses of human IL33 for 12 hours. The expression of REG3 α was determined by qRT-PCR, and normalized against GAPDH. Significance was calculated using 1-way ANOVA test (A, B, D-G), or Student t test (C). * $P < .05$; ** $P < .01$. Data are represented as means \pm standard deviation. One representative of 3-5 experiments with similar results.

generated IL33 knockout (IL33 KO) MSIE cells by CRISPR, and then treated WT and IL33 KO cells with IL33. Consistent with data from IL33 KO mice (Figure 1A), REG3 γ expression was greatly decreased in IL33 KO MSIE cells compared with WT cells. Interestingly, IL33 induced REG3 γ expression in IL33 KO MSIE cells at a lower level compared with WT MSIE cells (Figure 2D), indicating that IL33 stimulates production of itself in IEC as a positive loop to promote REG3 γ expression.

We then investigated if IL33 induces REG3 γ expression by IEC synergistically with IL17 and IL22, which have been shown previously to induce expression of REG3 γ in IEC.¹⁷ We treated MSIE with IL33 in the presence or absence of IL17 or IL22. Consistent with previous observations,¹⁷ treatment with IL17 or IL22 increased IEC expression of REG3 γ , which was further enhanced in the presence of IL33 (Figure 2E), indicating that IL33 induces REG3 γ synergistically with IL17 and IL22. To determine whether IL33 is involved in the IL17 and IL22 induction of REG3 γ in IEC, we administered WT and IL33 KO mice IL17 and IL22 intraperitoneally for 10 days. Interestingly, although IL17 and IL22 greatly promoted IEC expression of REG3 γ in WT mice, the levels of IL17- and IL22-induced IEC expression of REG3 γ were dramatically decreased in IL33^{-/-} mice (Figure 2F), indicating that induction of IEC REG3 γ expression by IL17 and IL22 is partially dependent on induction of IL33.

To determine if IL33 also regulates expression of REG3 in human IEC, a human colonic epithelial cell line, HT-29, was stimulated with IL33 for 12 hours. Consistently, mRNA expression level of REG3 α , the human ortholog of mouse REG3 γ , was enhanced in IL33-treated HT-29 cells in a dose-dependent manner (Figure 2G).

IL33 Induction of REG3 γ Was Mediated by mTOR, STAT3, and ERK1/2

We then explored the underlying mechanisms by which IL33 induces IEC expression of REG3 γ . We first measured the activation of STAT3, which has been shown to be crucial in the induction of REG3 γ ,^{18,19} in MSIE cells after treatment with IL33. IL33 treatment activated STAT3 as evidenced by enhanced expression of phosphorylated-STAT3 (p-STAT3) detected by Western blot analysis (Figure 3A).

To determine if activation of STAT3 mediates IL33-induction of REG3 γ in IEC, we inhibited STAT3 pathway by using complementary approaches, including using a STAT3 small molecule inhibitor, short interfering RNAs (siRNAs), and CRISPR. We then measured REG3 γ expression by qRT-PCR and Western blots. When the STAT3 inhibitor, HJC0152,²⁰ was added to the MSIE cell cultures with IL33, IL33-induction of REG3 γ was greatly reduced (Figure 3B). To further confirm these results, we transfected MSIE with STAT3 siRNA. Nontargeting siRNA was used as controls. Silencing STAT3 led to decreased REG3 γ mRNA expression and protein production in MSIE cells (Figure 3C and D). Consistently, knockout of STAT3 by CRISPR also inhibited IL33-induction of REG3 γ in IEC (Figure 3E and F). Together, these data indicated that STAT3 mediates IL33-induction of REG3 γ in IEC.

It has been shown that the mTOR and MEK-ERK pathways are required for the activation of STAT3.^{21,22} To investigate whether IL33 activates mTOR and MEK-ERK, we assessed levels of the phosphorylated-mTOR (p-mTOR) and the phosphorylated-ERK1/2 (p-ERK1/2) in MSIE cells after treatment with IL33. Indeed, IL33 treatment activated mTOR and ERK1/2 (Figure 3A). We then investigated if mTOR and ERK1/2 are also involved in IL33-induction of REG3 γ in IEC. Addition of mTOR inhibitor, AZD8055, or ERK1/2 inhibitor, U0126, into MSIE cell cultures inhibited the IL33-induced REG3 γ expression (Figure 3G and H). We next specifically silenced mTOR, and MEK1, the upstream kinases of ERK1, respectively, by siRNAs. Nontargeting siRNA was used as controls. As shown in Figure 3C and D, blockade of the mTOR and MEK1 pathways greatly inhibited IL33-induced REG3 γ expression, at both gene and protein levels, in MSIE cells. Knockout of mTORC1, MEK1, and MEK2 by CRISPR further confirmed these results (Figure 3E and F). These results thus indicated that mTOR and MEK-ERK1/2 were involved in IL33-induction of REG3 γ in IEC.

Next, we investigated how these 3 pathways interact to mediate IL33-induction of REG3 γ in IEC. We knocked out STAT3, mTOR, and MEK1/2 in MSIE cells by CRISPR individually, and then determined how knockout of 1 pathway affects the activation of others induced by IL33. As shown in Figure 4A–D, knockout of mTOR did not affect ERK1/2 activation but significantly inhibited STAT3 activation induced by IL33 as evidenced by decreased phospho-STAT3 by Western blots. Similarly, knockout of MEK2 did not affect mTOR activation but inhibited STAT3 activation. In contrast, knockout of STAT3 did not affect activation of mTOR and ERK1/2. Put all together, these data suggested mTOR and MEK acted as upstream regulators of STAT3 in IL33-induction of REG3 γ in IEC (Figure 4E).

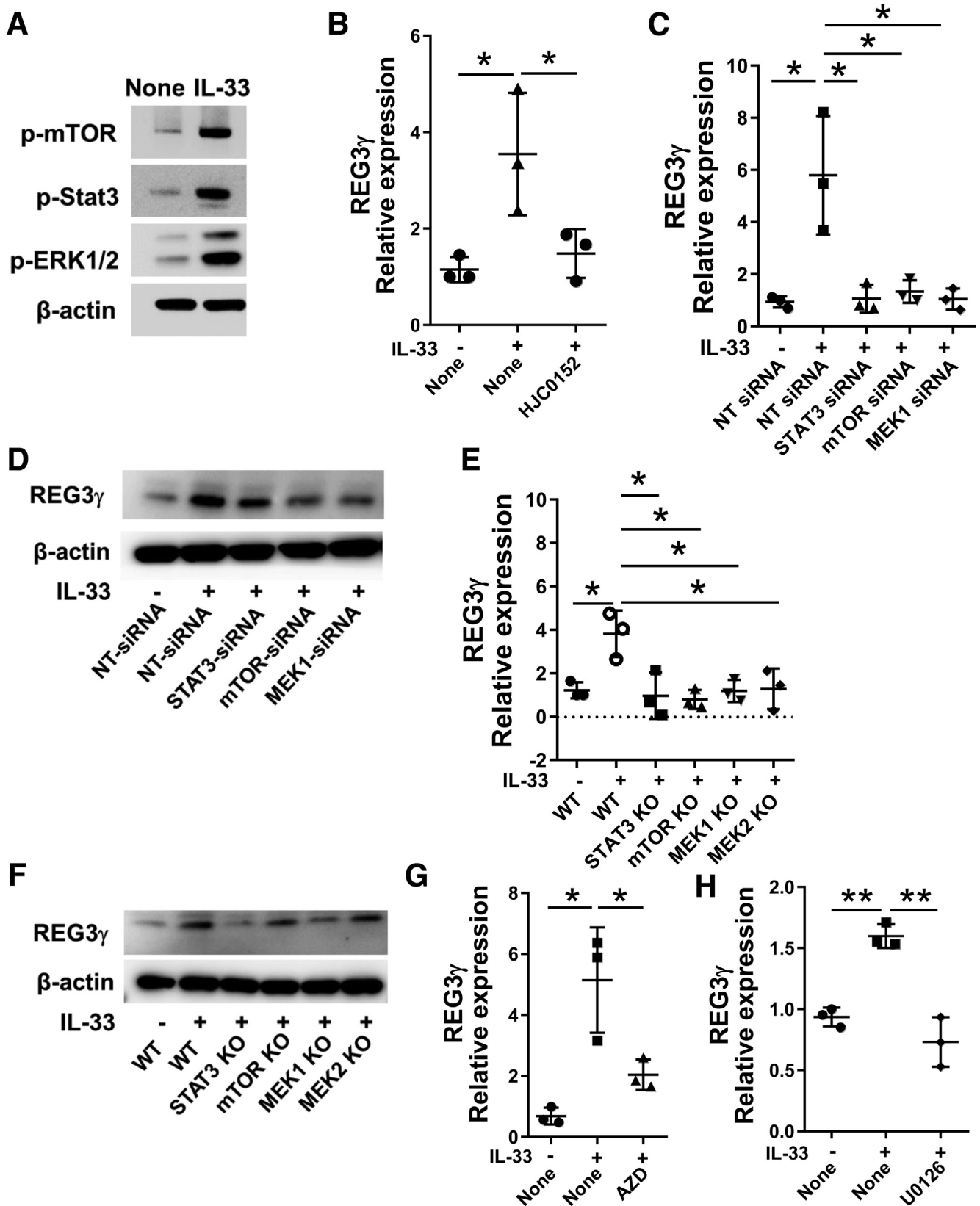
Because IL33 has been shown to be able to activate nuclear factor (NF)- κ B,^{23,24} we also investigated whether NF- κ B mediates IL33-induction of REG3 γ in IEC. We added Bay 11-7082, an NF- κ B inhibitor,²⁵ into the MSIE cultures along with IL33. The REG3 γ expression was not affected by Bay 11-7082 supplementation (Figure 5A), suggesting that IL33-induction of REG3 γ was not dependent on activation of NF- κ B. In addition, gene expression of cytokine signaling 3 (SOCS3), which is a negative regulator of STAT3,²⁶ and hypoxia-inducible factor 1 α (HIF-1 α), a downstream signaling molecule of mTOR,²⁷ was not affected by IL33 in MSIE cells (Figure 5B and C). It has been shown that IL33 administration promoted IL33 receptor (ST2) in splenic and thymic regulatory T cells in mice²⁸; however, the expression of ST2 was not regulated by IL33 in epithelial cells (Figure 5D).

IL33 Regulates the Gut Microbiota

Because REG3 γ has been shown to play crucial roles in maintaining intestinal homeostasis against microbiota, and our studies demonstrated that IL33 promoted IEC production of REG3 γ , we then determined if IL33 regulates gut microbiota under normal conditions. We first assessed the total gut microbiota by using the 16S gene expression

determined by qRT-PCR in WT and IL33^{-/-} mice. As shown in Figure 6A, the levels of gut bacteria were significantly higher in IL33^{-/-} mice than that of WT mice, indicating that

there was more gut microbiota in the absence of IL33, indicative of IL33 controlling gut microbiota under steady conditions. We next compared the composition of the fecal



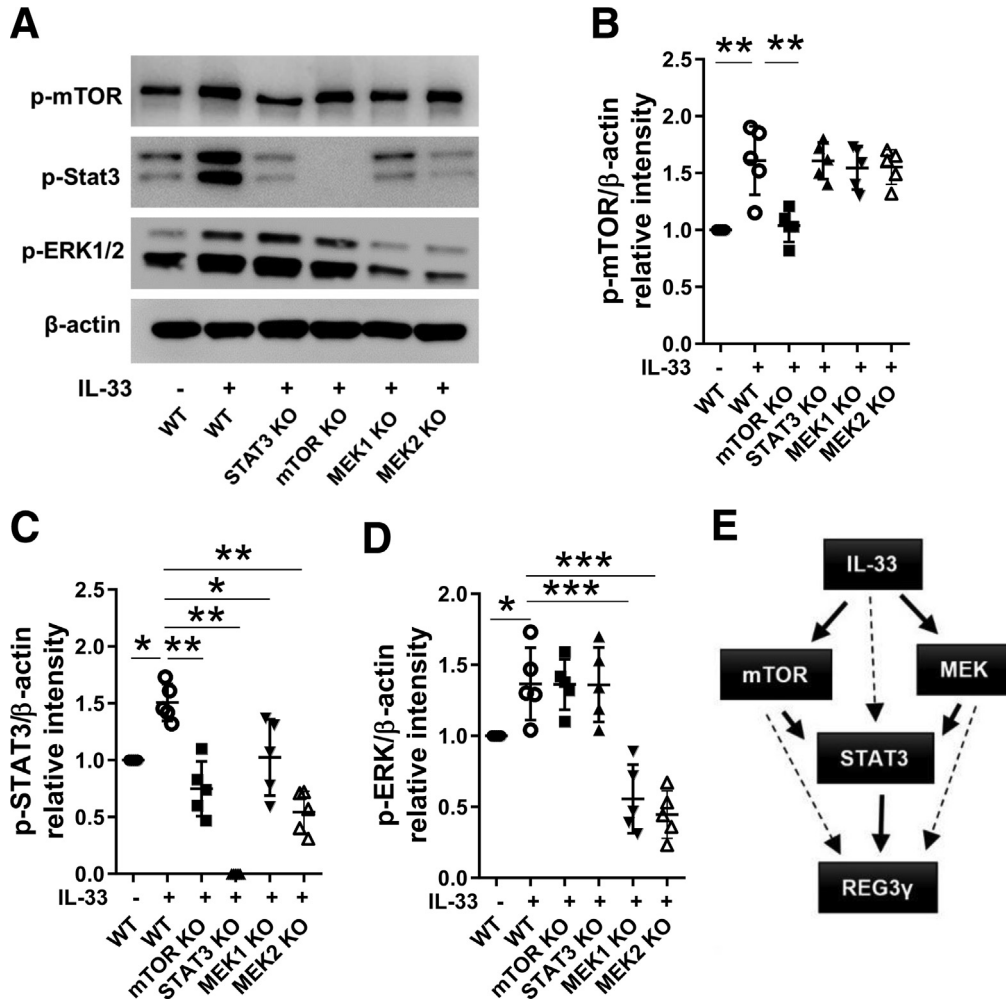


Figure 4. Interaction of STAT3, mTOR, MEK1, and MEK2 in IL33-induction of REG3 γ in IEC. STAT3, mTOR, and MEK2 were knocked out in MSIE cells by using CRISPR, and then treated with 10 ng/mL of IL33 for 15 minutes ($n = 3$). WT MSIE cells were also treated with IL33 ($n = 3$) as control. (A) The phosphorylated mTOR (pmTOR), STAT3 (pSTAT3), and ERK1/2 (pERK1/2) were determined by Western blot, with β -actin as a loading control. (B–D) Quantitative results of protein levels of pmTOR, pSTAT3, and pERK1/2 were analyzed using ImageJ software and was normalized against β -actin. (E) Summary diagram demonstrating the interaction of mTOR, ERK2, and STAT3 in IL33 induction of REG3 γ in IEC. Significance was calculated using 1-way analysis of variance test. * $P < .05$; ** $P < .01$, *** $P < .001$. Data were pooled from 5 experiments, and shown as means \pm standard deviation.

bacterial communities of IL33 $^{-/-}$ and WT mice by using 16S rRNA pyrosequencing analysis. The principal coordinates based on an unweighted UniFrac principal coordinate analysis clearly separated the samples from the 2 mouse

lines (Figure 6B), indicating that the composition of the fecal bacterial community was altered by deficiency of IL33. Taxonomically, differences in the microbial distributions of WT and IL33 $^{-/-}$ mice were found at classifications from

Figure 3. (See previous page). IL33 activates mTOR, STAT3, and ERK1/2 in IEC. (A) MSIE cells were treated with 10 ng/mL of IL33. Phosphorylated STAT3 (pSTAT3, 4 hours), phosphorylated mTOR (pmTOR, 4 hours), and phosphorylated ERK1/2 (pERK1/2, 4 hours) were determined by Western blot, with β -actin as a loading control. (B) MSIE cells ($n = 3$ wells/group) were treated with 10 ng/mL of IL33 in the presence or absence of STAT3 inhibitor, HJC0152, and the expression of REG3 γ was determined by qRT-PCR and normalized against glyceraldehyde-3-phosphate dehydrogenase (phosphorylating) (GAPDH). (C–F) STAT3, mTOR, MEK1, and/or MEK2 were knocked down in MSIE cells by siRNA (C, D), and knocked out by CRISPR (E, F), and the cells were then treated with 10 ng/mL of IL33 for 12 hours ($n = 3$ wells/group). WT MSIE cells were included ($n = 3$ wells/group) as control. The expression of REG3 γ was determined by qRT-PCR and normalized against GAPDH (C, E). The protein levels of REG3 γ were determined by Western blot analysis, with β -actin as a loading control (D, F). MSIE cells ($n = 3$ wells/group) were treated with 10 ng/mL of IL33 in the presence or absence of mTOR inhibitor AZD8055 (G), or MEK inhibitor U0126 (H), and the expression of REG3 γ was determined by qRT-PCR and normalized against GAPDH. Significance was calculated using 1-way analysis of variance test. * $P < .05$; ** $P < .01$. Data are represented as means \pm standard deviation. One representative of 3–5 experiments with similar results.

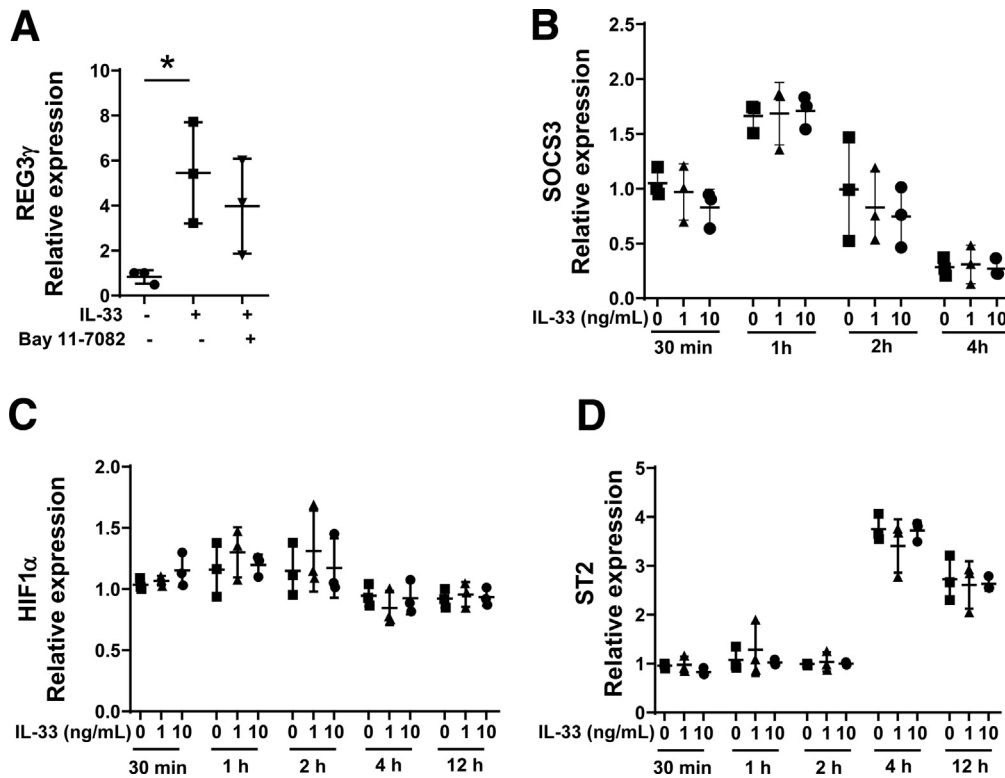


Figure 5. IL33 induction of REG3 γ is not dependent on NF- κ B activation, and IL33 has no effect on SOCS3, HIF1 α , and ST2 expression in IEC. (A) MSIE cells ($n = 3$ wells/group) were treated with 10 ng/mL of IL33 in the presence or absence of NF- κ B inhibitor, Bay 11-7082. The expression of REG3 γ was determined by qRT-PCR and normalized against glyceraldehyde-3-phosphate dehydrogenase (phosphorylating). (B–D) MSIE cells ($n = 3$ wells/group) were treated with IL33 (10 ng/mL) at different time points. The expression of SOCS3 (B), HIF1 α (C), and ST2 (D) were determined by qRT-PCR and normalized against glyceraldehyde-3-phosphate dehydrogenase (phosphorylating). Significance was calculated by 1-way analysis of variance test. * $P < .05$. Data are represented as means \pm standard deviation. One representative of 3–4 experiments with similar results.

phylum to genus. At the genus level (Figure 6C), IL33 deficiency led to increased levels of *Alistipes*, *Bacteroides*, *Ruminococcus*, *Ruminiclostridium*, and *Lachnospiraceae* NK4A136 group (Figure 6D–H), whereas *Desulfovibrio* and *Mucispirillum* was substantially decreased in IL33 $^{-/-}$ mice (Figure 6I and J).

IL33 Inhibits Bacterial Colonization in the Intestines

To further investigate whether IL33 deficiency affects gut bacterial colonization, we infected WT and IL33 $^{-/-}$ mice with *C rodentium*, a enteric bacterial strain that has been widely used to induce a transient distal colitis in mice.²⁹ We collected the feces at Day 7, 14, and 21 after infection, and performed an agar-plate culture for *C rodentium* count. Colony counts of the fecal *C rodentium* were higher in the IL33 $^{-/-}$ mice compared with WT control animals at Day 14 (Figure 7A), suggesting that IL33 controls colonization of *C rodentium* in vivo. To determine whether *C rodentium* infection triggers IL33 production by IECs, we assessed IEC IL33 expression after *C rodentium* infection by qRT-PCR. *C rodentium* infection promoted IEC expression of IL33 (Figure 7B). Consistently, treatment with *C rodentium*

antigen also increased IL33 expression by MSIE cells (Figure 7C). To investigate whether altered microbiota in IL33 $^{-/-}$ mice contributes the difference of *C rodentium* clearance, we cohoused IL33 $^{-/-}$ mice and WT littermates at weaning (3 weeks old) and infected them with *C rodentium* at 6–8 weeks old to potentially limit the effects of microbiota difference. The fecal *C rodentium* load was only detected in IL33 $^{-/-}$ mice at Day 17 with lower REG3 γ expression in IEC but not in WT mice (Figure 7D and E).

IL33-Treated IEC Inhibits Bacterial Growth In Vitro Partially Through Induction of REG3 γ

To further determine the mechanisms by which IL33 controls *C rodentium*, we conducted the antibacterial experiments by culturing *C rodentium* with the crude extracts of MSIE cells pretreated with or without IL33. We also added IL33 alone to *C rodentium* culture to determine if IL33 can directly kill *C rodentium*. IL33 alone did not affect the growth of *C rodentium* (Figure 7F). However, after cultured with the crude extracts from IL33-treated MSIE cells, the growth of *C rodentium* was inhibited compared with that with the extracts from control MSIE cells at both 12 hours and 18 hours (Figure 7G). We then investigated

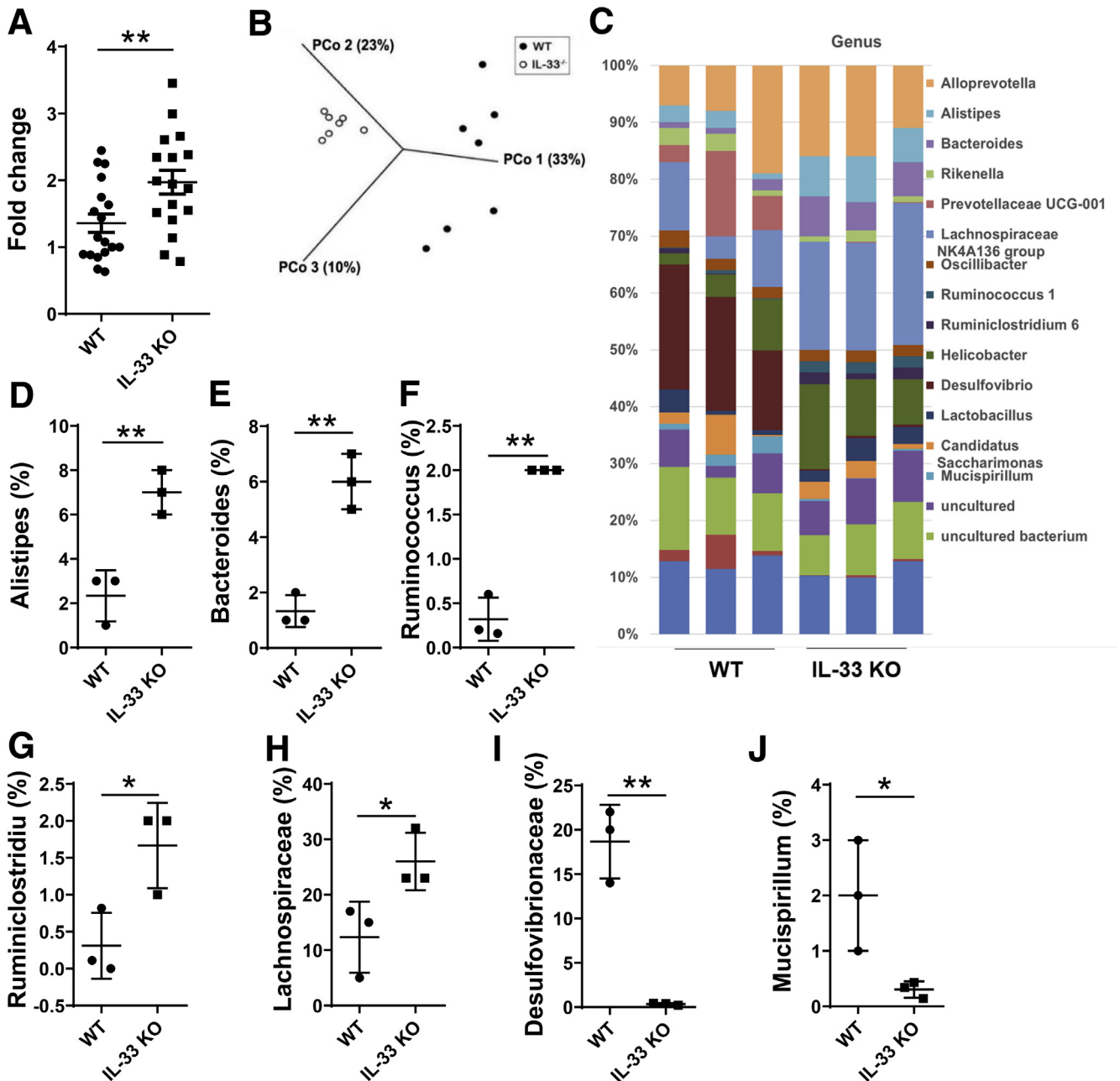


Figure 6. Increased total gut microbiota and altered composition of gut bacterial communities in IL33^{-/-} mice. Fecal bacterial DNA was prepared from WT and IL33^{-/-} mice. (A) Total bacteria (n = 17 mice/group) were determined by measuring 16S rDNA using qRT-PCR, and data was normalized to eukaryotic β -actin. (B, C) 16S rDNA pyrosequencing was performed. Principal Coordinates Analysis of unweighted UniFrac distances for 16S rDNA V3–V4 sequence data of gut microbiota in WT and IL33^{-/-} mice (n = 7/group) (B). Differences in the microbial distributions of WT and IL33^{-/-} mice (n = 3/group) were found at the genus level (C). The percentages of *Alistipes* (D), *Bacteroides* (E), *Ruminococcus* (F), *Ruminiclostridium* (G), *Lachnospiraceae* NK4A136 group (H), *Desulfovibrio* (I), and *Mucispirillum* (J) in the total bacteria in the feces of WT and IL33^{-/-} mice, respectively. Significance was calculated using Student *t* test. **P* < .05. ***P* < .01. Data are represented as means \pm standard deviation.

whether induction of REG3 γ by IL33 regulates the inhibitory effects on bacteria. To this end, we generated REG3 γ knockout (REG3 γ KO) MSIE cells by CRISPR, and then treated WT and REG3 γ KO MSIE cells with IL33. The extracts of the cells were then added to the culture of *C. rodentium*. As shown in Figure 7G and H, although IL33

treatment promoted WT IEC inhibition of *C. rodentium*, it did not promote REG3 γ KO IEC inhibition of the bacteria. Moreover, REG3 γ KO IEC allowed more *C. rodentium* growth compared with WT IEC (Figures 7I), indicating that the IEC production of REG3 γ induced by IL33 plays a key role in inhibition of *C. rodentium* growth. Taken together,

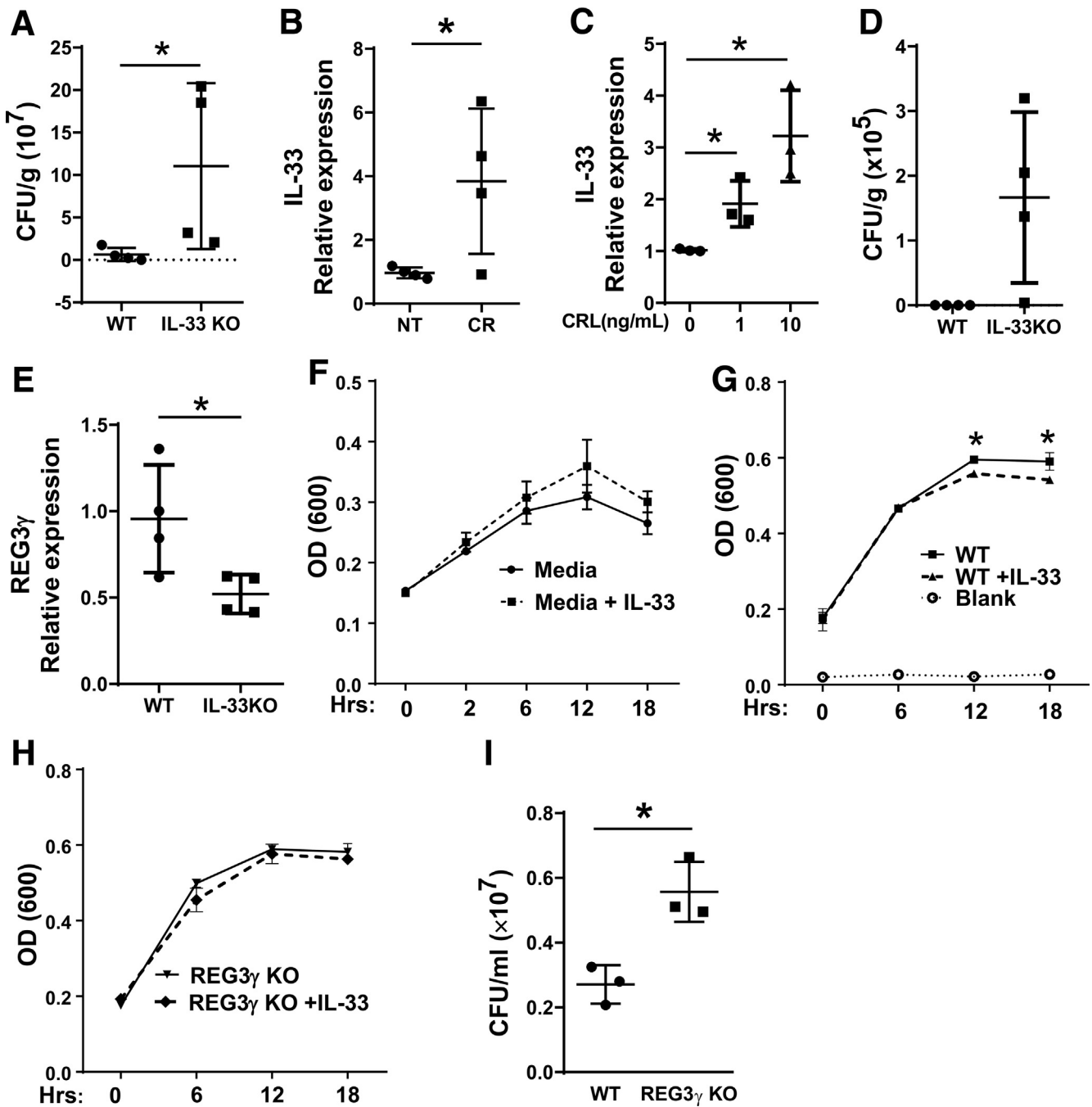


Figure 7. IL33 promotes IEC killing of *Citrobacter rodentium*. (A-B) WT and IL33^{-/-} mice (n = 4/group) were orally infected with *C. rodentium*. Total counts of fecal *C. rodentium* were determined at Day 14 (A), and IEC expression of IL33 was determined by qRT-PCR and normalized against glyceraldehyde-3-phosphate dehydrogenase (phosphorylating) (GAPDH) (B). (C) MSIE cells (n = 3 wells/group) were treated with *C. rodentium* lysates at different dose for 6 hours, the expression of IL33 was determined by qRT-PCR and normalized against GAPDH. (D, E) IL33^{-/-} mice and WT littermates (n = 4/group) were cohoused at weaning and infected with *C. rodentium* orally at 6–8 weeks old. Total counts of fecal *C. rodentium* were determined at Day 17 (D), and IEC expression of IL33 was determined by qRT-PCR and normalized against GAPDH (E). *C. rodentium* were cultured with media alone with or without IL33 (n = 3 wells/group) (F), or the crude extracts of WT (G) and REG3 γ KO (H) MSIE cells (n = 3 wells/group) that were pretreated with or without IL33. The OD values (600 nm) were measured at different time points. (I) After treated with the extracts of IL33-pretreated WT or REG3 γ KO MSIE cells (18 hours) (n = 3 wells/group), bacteria culture suspensions were colonized to solid culture plates for colony counting. Significance was calculated using Student *t* test. **P* < .05. Data are represented as means \pm standard deviation. One representative of 3–5 experiments with similar results. CR, *Citrobacter rodentium*; CRL, *Citrobacter rodentium* lysates.

these data indicated that IL33 promoted IEC clearance of *C rodentium*, which is at least partially mediated by induction of REG3 γ .

Discussion

It has been shown that the expression of mucosal IL33, localized primarily to IEC, is increased during inflammation and mucosal wound healing.^{30,31} Under such conditions, epithelial-derived IL33 triggers both T-helper cell type 1 and T-helper cell type 2 inflammatory responses via the IL33/ST2 axis.³² Although epithelial cells have generally been identified as a primary source of IL33, very few studies have been conducted to examine whether IL33, in turn, regulates the function of epithelial cells, the primary producers of IL33 in the intestines. Antimicrobial proteins and peptides are also produced by epithelial cells, and play important roles in host antimicrobial defense during intestinal homeostasis and inflammation.³³ In this study, we explored the possible connection between IL33 and epithelial-produced AMPs for the first time. Our data from both *in vitro* and *in vivo* studies demonstrated that IL33 induced the expression of REG3 γ in IEC and contributed to gut microbiota symbiosis, thus providing a novel self-regulatory mechanism for IEC in protecting themselves by producing IL33.

It has been reported that under steady conditions, endothelial cells in blood vessels and epithelial cells at various barrier tissues express IL33 constitutively.^{8,15} It can be released on stimulation by multiple factors, including TLR ligands. Because intestines host huge amounts of microbiota, it would not be surprising that some of IL33 stimulators are produced by gut microbiota constantly, even at very low concentration. This would serve as 1 of regulatory mechanisms that regulate intestinal homeostasis against microbiota. Indeed, by using enzyme-linked immunosorbent assay and Western blots, we did detect a measurable level of IL33, which could be readily released on stimulation by gut microbiota products. Constant production of IL33 *in vivo*, even at low levels, functions on various cells. Our study also demonstrated a loop of IL33 promoting production of itself to inducing REG3 γ , in that IL33 induced Reg3 γ expression by IL33 KO IEC at lower levels compared with that in WT IEC.

The role of IL33 in regulation of intestinal homeostasis is still not completely clear because protective and pathogenic functions have been reported in different experimental settings.^{12,14,34–36} Among many factors contributing to such controversial reports, differences in gut microbiota between different animal facilities could be a major confounding factor. Our current study demonstrated that IL33 controls total gut microbiota and the composition of gut microbiota, as determined by 16s rDNA sequencing analysis in IL33-deficient mice. Furthermore, IL33 limits the survival of ingested microbes, such as *C rodentium in vivo*. Because IL33 did not directly kill or inhibit the growth of bacteria, this was likely mediated by IL33 promotion of IEC defense against gut bacteria, as IL33 treatment enhanced IEC clearance of bacteria. REG3 γ has been considered as an

important regulatory factor of intestinal microbiota because of its bactericidal activity against gut bacteria. It has also been shown that REG3 γ has a protective role against infection with pathogenic *Salmonella* and *Listeria* in mice.³⁷ Interestingly, knocking out of REG3 γ in IEC decreased the capability of IEC-facilitated clearance of *C rodentium* induced by IL33, indicating that REG3 γ mediated, at least partially, IL33-induced IEC defense against bacteria. Although when cohoused with WT littermates at weaning, which potentially limits the effects of microbiota difference, IL33^{-/-} mice still demonstrated the impaired *C rodentium* clearance, our data did not directly address whether the response to *C rodentium* infection in IL33 KO mice is caused by the difference in microbiota composition. Thus, the impaired bacteria clearance in IL33^{-/-} mice could be at least partially caused by dysregulated IL33 regulation of Reg3 γ expression. Our *in vitro* data showed that IL33-treated IEC controlled *C rodentium* growth, which was mediated by IL33-induced Reg3 γ , and independent of microbiota because there was no microbiota in that *in vitro* culture system. Although these data do not exclude the roles of altered microbiota or the roles of other types of cells could affect *C rodentium* infection *in vivo*, our study indeed demonstrated the roles of IL33-IEC-Reg3 γ axis in regulation of *C rodentium* infection. The hosts have developed multiple mechanisms controlling infection, intestinal injury, and constant exposure to microbiota. Many regulatory mechanisms involve self-regulation. We demonstrated that *C rodentium* infection promoted IEC expression of IL33, which in turn promoted IEC expression of Reg3 γ to control *C rodentium* infection, thus providing a novel self-regulatory mechanism in controlling intestinal homeostasis and enteric infection.

Although substantial progress has been made in the last several years, the exact signaling pathways mediating IEC production of REG3 γ are still not completely understood. We demonstrated here that IL33 activated STAT3 in IEC, and inhibition of STAT3 impaired IL33-induction of REG3 γ in IEC, indicating that STAT3 mediated IL33-induction of REG3 γ in IEC, which is consistent with a previous report.¹⁸ Interestingly, IL33 also activated mTOR and MEK-ERK pathways in IEC, and knockout of each these pathways inhibited IL33-induction of REG3 γ in IEC, indicating that the mTOR and MEK-ERK pathways are also involved in IL33-induction of REG3 γ in IEC. However, IL33 did not affect SOCS3, an important feedback inhibitor of the STAT3 pathway,³⁸ suggesting that the regulation of STAT3 by IL33 is not via the STAT3/SOCS3 axis. NF- κ B is activated by IL33.^{23,24} Although there is little evidence that NF- κ B directly regulates the expression of AMPs, some AMPs, such as human β -defensin-2, are regulated by TLR4- and TLR2-dependent pathways, which require NF- κ B trans-activation.³⁹ However, our data indicated that IL33-induction of REG3 γ in IEC was NF- κ B-independent.

Our studies demonstrated that mTOR, STAT3, and ERK1/2 were all involved in mediating IL33-induction of REG3 γ in IEC. These findings raised the questions about how these pathways act; namely, do they act independently or work together in that matter? Although it has been

shown that the mTOR pathway was mediated by ERK in human keratinocytes,⁴⁰ and in mouse osteoblastic cells,⁴¹ we showed that mTOR and ERK1/2 were 2 independent pathways in IL33-induction of REG3 γ in IEC. Specifically, knocking out mTOR did not affect activation of MEK1/2 in IEC treated with IL33, and vice versa, knocking out MEK1/2 did not affect activation of mTOR. However, STAT3 activation was inhibited by knocking out either mTOR or MEK2, indicating that mTOR and MEK2 are the upstream pathways of STAT3 in IL33-induction of REG3 γ in IEC. This is consistent with a previous report that showed that mTOR was able to regulate STAT3 pathway.⁴² Although a previous study suggested STAT3 serine phosphorylation can be mediated by both ERK-dependent and-independent pathways,⁴³ we demonstrated that the phosphorylation of STAT3 is MEK2-dependent in IL33-induction of REG3 γ in IEC. However, it is still unclear whether IL33 directly activates STAT3, because our current data cannot exclude such possibility.

In summary, our study demonstrated that IL33, which is produced by IEC in response to injury and inflammatory stimulation, in turn, promotes IEC expression of REG3 γ , and controls the gut microbiota of the host. We, thus, identified a novel self-regulatory mechanism in controlling intestinal homeostasis in which IEC produces IL33 to protect themselves against the overwhelming invasion of gut microbiota.

Materials and Methods

Mice

C57BL/6 mice were purchased from the Jackson Laboratory (Bar Harbor, ME). IL33^{-/-} mice on C57BL/6 background were kindly provided by Dr. Rene de Waal Malefyt (Merck, Palo Alto, CA), and bred with WT C57BL/6 mice. WT and IL33^{-/-} littermates were cohoused and used as indicated in the text. All mice were housed under specific pathogen-free conditions at the animal resource center of University of Texas Medical Branch at Galveston. All experiments were reviewed and approved by the Institutional Animal Care and Use Committee of University of Texas Medical Branch at Galveston.

Reagents

Recombinant mouse IL33 (Cat# 580506, Lot# B223648), recombinant mouse interferon- γ (Cat# 575306, Lot# B203843), recombinant mouse IL17A (Cat# 576008, Lot# B252851), and recombinant mouse IL22 (Cat# 576208, Lot# B208032) was purchased from BioLegend (San Diego, CA). Culture medium RPMI 1640 (Cat# SH30027.01, Lot# AD16492263), penicillin/streptomycin (Cat# SV30010, Lot# J170049), and Percoll (Cat# 17089101, Lot# 10253323) were purchased from GE healthcare (Waukesha, WI). ITS (Cat# 354350, Lot# 15918002), HEPES (Cat# 25-060-CI, Lot# 08617003), EDTA (Cat# 46-034-CI, Lot# 08816016), and Matrigel (Cat# 356231, Lot# 7142014) were purchased from Corning (Corning, NY). B-27 Supplement ($\times 50$) (Cat# 17504-044, Lot# 2004383), DMEM/F12 (Cat# 12634-010, Lot# AC12854278), OPTI-MEM (Cat# 31985062, Lot# 1967528), Lipofectamine RNAiMAX Transfection Reagent (Cat# 13778150, Lot# 1815569), and NuPAGE Bis-Tris mini gels (Cat# NP0323PK2, Lot#

17060670) were purchased from Thermo Fisher Scientific (Waltham, MA). STAT3 inhibitor HJC0152 was kindly provided by Dr. Jia Zhou, University of Texas Medical Branch at Galveston. AZD8055 (Cat# S1555, Lot# 7) was purchased from Selleckchem (Houston, TX). MEK inhibitor, and U0126 (Cat# U120, Lot# 078K4623V) was purchased from Sigma Aldrich (St. Louis, MO). Predesigned siRNA directed against mouse mTOR (Cat# SI01005683, Lot# 211369750), STAT3 (Cat# SI01435287, Lot# 211309675), and negative control siRNA (Cat# 1027310, Lot# 208993226) were purchased from Qiagen (Hilden, Germany). SMARTpool siRNAs specific for murine MEK1 (Cat# L-040605-00, Lot# 110217) and nontargeting siRNA (Cat# D-001810-10-05, Lot# 1634172) were purchased from Dharmacon (Lafayette, CO). Western blot antibodies against phosphorylated STAT3 (Y705, Cat# 9145, Lot# 31), phosphorylated mTOR (S2448, Cat# 2971, Lot# 19), phosphorylated ERK1/2 (137F5, Cat# 4695, Lot# 8), β -actin (Cat# 8457, Lot# 7), and antirabbit secondary antibody conjugated with horseradish peroxidase (Cat# 7074, Lot# 28) were purchased from Cell Signaling Technology (Danvers, MA). Antibody against REG3 γ (Cat# ab198216, Lot# GR209823-25) was purchased from Abcam (Cambridge, MA). Recombinant mouse EGF protein (rEGF) (Cat# 2028-EG, Lot# MKG1117011), recombinant mouse Noggin protein (rNoggin) (Cat# 1967-NG/CF, Lot# ETY3115031), recombinant mouse R-Spondin 1 Protein (rR-spondin) (Cat# 3474-RS, Lot# OH04617071), recombinant human Wnt3a protein (rWnt3a) (Cat# 5036-WN/CF, Lot# RSK7816121), and N-2 MAX media supplement ($\times 100$) (Cat# AR009, Lot# 1421266) for enteroid culture were purchased from R&D Systems (Minneapolis, MN).

Isolation of IEC

The intestines were removed from the euthanized mice, cut into small segments, and rinsed thoroughly with cold phosphate-buffered saline (PBS). After incubating in PBS containing 0.5 mM EDTA at 37°C for 40 minutes under slow rotation, the epithelial layer was pooled and passed through a 100- μ m strainer (Cat# 120-018-899, Lot# 5150310608, Miltenyi Biotec, San Diego, CA). The pellet of epithelial cells was layered on 20%–40% gradient Percoll-RPMI solution, and centrifuged at 2000 rpm for 20 minutes at 25°C. IEC were collected from the interphase.

Epithelial Cell Culture

MSIE cells were cultured in RPMI 1640 medium with 5 U/mL murine interferon- γ , ITS (5 μ g/mL insulin, 5 μ g/mL transferrin, and 5 ng/mL selenous acid), 100 U/mL penicillin/streptomycin, and 5% fetal-bovine serum at 33°C. Before treated with IL33, MSIE cells were starved in RPMI 1640 media with 0.5% fetal-bovine serum and 100 U/mL penicillin/streptomycin for 16 hours. IL33 treatments were performed at 37°C; dosage and duration are described in the text.

Enteroid Culture

The small intestines were cut, minced, and treated with 2 mM EDTA, and then treated with 43.3 mM sucrose and 54.9

mM sorbitol in cold PBS. After filtering through a 70- μ m cell strainer, the supernatant was collected and centrifuged. The pellets containing detached crypts were resuspended in Matrigel with 0.5 μ g/mL rEGF, 1 μ g/mL rNoggin, 5 μ g/mL rR-spondin, and 1 μ g/mL rWnt3a. Matrigel of 50 μ l with 500 crypts was plated, and cultured in 500 μ L advanced DMEM/F12 medium supplemented with 1 \times N2, and 1 \times B27 for 5 days.

siRNA Transfection

siRNA transfection in MSIE cells was performed by using Lipofectamine RNAiMAX Transfection Reagent according to the manufacturer's instructions. The 2 \times 10⁵ MSIE cells were incubated with 30 pmol siRNA and 3 μ L Lipofectamine RNAiMAX transfection reagent in 1 mL per well OPTI-MEM

medium for 6 hours in a 24-well plate, followed by replacing with 1 mL normal medium per well for 24 hours at 33°C. Transfection efficiency was determined at 24 hours post transfection. MSIE cells were then cultured in serum-starved conditions for 16 hours at 33°C before treatment. The treatments were performed at 37°C; dosage and duration are described in the text.

Quantitative Real-Time PCR

Total RNA was extracted with TRIzol (Cat# 15596018, Lot# 74101, Life Technologies, Waltham, MA) and quantified for cDNA synthesis. qRT-PCR reactions were performed by using SYBR Green Gene Expression Assays (Cat# 1725124, Lot# 64201094, Bio-Rad, Hercules, CA). The primers used for SYBR Green system are listed in Table 1. Predesigned primers

Table 1. PCR Primers and CRISPR-Guide RNA Oligo Sequences

PCR primers		
mGAPDH	Forward	5'- TCAACAGCAACTCCCCTCTTCCA-3'
	Reverse	5'- ACCCTGTTGCTGTAGCCGTATTCA-3
mRegIII γ	Forward	5'-ATGCTTCCCCGTATAACCATCA-3'
	Reverse	5'-ACTTCACCTTGCACCTGAGAA-3'
m β -defensin-1	Forward	5'- CCAGATGGAGCCAGGTGTTG-3'
	Reverse	5'- AGCTGGAGCGGAGACAGAATCC-3'
m β -defensin-3	Forward	5'- AAAGGAGGCAGATGCTGGAA-3'
	Reverse	5'- ACGGGATCTTGGTCTTCTCT-3'
m β -defensin-4	Forward	5'- GCAGCCTTTACCCAAATTATC-3'
	Reverse	5'- ACAATTGCCAATCTGTGCGAA-3
mIL33	Forward	5'-GCTGCGTCTGTTGACACATT-3'
	Reverse	5'-CACCTGGTCTTGCTCTTGGT-3'
mHIF-1 α	Forward	5'-AGCTTCTGTTATGAGGCTCACC-3'
	Reverse	5'-TGACTTGATGTTTCATCGTCCTC-3'
mST-2	Forward	5'-CATGGCATGATAAGGCACAC-3'
	Reverse	5'-GTAGAGCTTGCCATCGTTCC-3'
hGAPDH	Forward	5'- CAGGAGGCATTGCTGATGAT-3'
	Reverse	5'- GAAGGCTGGGGCTCATT-3'
hRegIII α	Forward	5'-TATGGTCCCCTGCTATGCCT-3'
	Reverse	5'-TCTTACCAGGGAGGACACGAA-3'
CRISPR-guide RNA oligo sequences		
STAT3	Forward	5' – CACCGCGATTACCTGCACTCGCTTC – 3'
	Reverse	5' – AAACGAAGCGAGTGCAGGTAATCGC – 3'
mTOR	Forward	5' – CACCGTGATACGAACTAGCTCGTTG– 3'
	Reverse	5' – AAACCAACGAGCTAGTTCTGATCAC– 3'
MEK1	Forward	5' – CACCGCTTGTGCTTCTCCGAAGAT– 3'
	Reverse	5' – AAACATCTTCGGGAGAAGCACAAGC– 3'
MEK2	Forward	5' – CACCGATGATCTGGTTGCGCACGGC– 3'
	Reverse	5' – AAACGCCGTGCGCAACCAGATCATC– 3'
REG3 γ	Forward	5' – CACCGTAGGGCTATGAACCCAACAG– 3'
	Reverse	5' – AAACCTGTTGGGTTTCATAGCCCTAC– 3'
IL33	Forward	5' – CACCGTGATCAATGTTGACGACTC– 3'
	Reverse	5' – AAACGAGTCGTCAACATTGATCAC– 3'
ST-2	Forward	5' – CACCGTTGATGTACTCGACAGTACG– 3'
	Reverse	5' – AAACCGTACTGTGAGTACATCAAC– 3'

PCR, polymerase chain reaction.

and probes for SOCS3 (Mm01249173_g1, Cat# 4331182, Lot# 1257861) and glyceraldehyde-3-phosphate dehydrogenase (phosphorylating) (Mm99999915_g1, Cat# 4331182, Lot# P121105-000) were purchased from Applied Biosystems (Waltham, MA). Quantitative PCRs were performed by using TaqMan Gene Expression Assays (Cat# 1725285, Lot# 720001365, Bio-Rad). All data were normalized to glyceraldehyde-3-phosphate dehydrogenase (phosphorylating) mRNA expression.

Western Blot

The total protein of the cells was isolated through radioimmunoprecipitation assay with phenylmethanesulphonyl, protease inhibitor cocktail, and phosphatase inhibitors. The concentration was determined using a BCA Protein Assay kit. A total of 6 μ g of protein was separated electrophoretically by NuPAGE Bis-Tris mini gels and probed with REG3 γ , phospho-mTOR, phospho-STAT3, phospho-MEK1, and phospho-MEK2 primary Abs, followed by incubation with a horseradish peroxidase-conjugated antirabbit secondary antibody. The bands were detected by enhanced chemiluminescence assay (Cat# 34080, Lot# RJ238638B, Thermo Fisher Scientific).

Knockout of IL33, ST2, STAT3, mTOR, MEK, and REG3 γ by Using CRISPR

The CRISPR/Cas9 system, lentiCRISPR v2 (Addgene plasmid # 52961), was established by the Zhang laboratory.⁴⁴ The design and cloning of the target guide RNA sequences was performed as recommended by the Zhang laboratory GeCKO Web site (<http://www.genome-engineering.org>). Briefly, the suitable target sites for guide RNA sequence against STAT3, mTOR, MEK, REG3 γ , IL33 and ST2 were identified by using CRISPR design tool software at <http://crispr.mit.edu>. Cas9-target sites for the indicated genes were designed in <http://crispr.genome-engineering.org>. The synthetic guide RNAs (Integrated DNA Technologies, Coralville, IA) containing target sites were subcloned into the lentiCRISPR v2 vector, and transfected into MSIE cells. After antibiotic positive selection, cells were established as a stable cell line. Guide RNA oligo sequences for lentiCRISPR v2 are listed in Table 1.

qRT-PCR for Bacterial 16S rDNA

Fecal pellets were collected and fecal DNA was extracted using PowerSoil DNA Isolation Kit (Cat# 12888-50, Lot# 160021967, Qiagen). Relative quantification of bacteria was performed by qRT-PCR using the primers targeting 16S ribosome (Fwd: TCCTACGGGAGGCAGCAGT, Rev: GGACTAC-CAGGGTATCTAATCTGTT), and data were normalized to eukaryotic β -actin.

16S rRNA Pyrosequencing Analysis

Fecal bacterial DNA was isolated using a QIAAMP PowerFecal DNA kit (Cat# 12830-50, Lot# 160044775, Qiagen) according to the manufacturer guidelines. The isolated DNA was amplified using universal V3-V4 16S

rRNA V3-V4 region primers.⁴⁵ Sequencing was performed with an Illumina MiSeq instrument in 2 sequencing runs resulting in 35,000–105,000 base pair paired reads according to the manufacturer guidelines. The raw sequencing reads were trimmed and filtered based on initial quality assessment using CLC Genomics Workbench 10.0.1. To identify the presence of known bacteria, the subsequences were analyzed using CLC Genomics Workbench 10.0.1 Microbial Genomics Module. Reference based OTU picking was performed using the SILVA SSU v119 97% database.⁴⁶ Sequences present in more than 1 copy without assigned taxa using with above were placed into *de novo* OTUs (97% similarity) and aligned against the database with 80% similarity threshold using MUSCLE alignment. As result, 1156 taxonomic units were identified based on 325,886 total reads excluding singletons.

Citrobacter rodentium Infections

C. rodentium strain DBS100 (ATCC) was grown overnight in Luria-Bertani broth at 37°C and subcultured (1:100 dilution) in fresh broth for 4–5 hours. Adult mice (6–8 weeks old) were infected with 200 μ L of bacterial suspension (5×10^8 bacteria) by oral gavage. At Day 7, 14, and 17, fecal pellets were collected from individual mice, weighed, and homogenized in 5 mL of PBS. Serial dilutions of the homogenates were plated onto MacConkey's agar (Cat# 211387, Lot# 7076631, BD Biosciences, San Jose, CA), and CFU per gram of fecal pellets were counted after overnight incubation.

In Vitro Killing of Bacteria by the Protein Extracts of IL33-Treated MSIE Cells

WT and REG3 γ knockout MSIE cells were cultured with or without IL33 for 18 hours, then crude protein was extracted from cells in RPMI-1640 media supplemented with 1 mM PMSF. The protein concentration of the extracts in each group was diluted to 1.2 mg/mL. *C. rodentium* strain DBS100 (ATCC) was added MSIE extracts or control media with an initial OD (600 nm) of 0.1–0.2. The bacteria cultures were kept at 37°C for up to 18 hours in aerobic condition. Then the bacteria culture suspensions were colonized to solid culture plates overnight for colony counting. MacConkey's agar plates were used for *C. rodentium* growth.

Statistical Analysis

Student *t* test was used to determine levels of significance for comparisons between samples by using Graphpad Prism 6.0 software. Student *t* test was used to determine levels of significance for comparisons between 2 groups, and 1-way analysis of variance test was performed to analyze the difference among groups by using Graphpad Prism 5.0 software. Results are shown as mean \pm standard deviation. Statistical significance is indicated as follows: **P* < .05; ***P* < .01.

References

- Artis D. Epithelial-cell recognition of commensal bacteria and maintenance of immune homeostasis in the gut. *Nat Rev Immunol* 2008;8:411–420.
- Goto Y, Ivanov II. Intestinal epithelial cells as mediators of the commensal-host immune crosstalk. *Immunol Cell Biol* 2013;91:204–214.
- Sun M, He C, Cong Y, Liu Z. Regulatory immune cells in regulation of intestinal inflammatory response to microbiota. *Mucosal Immunol* 2015;8:969–978.
- Gallo RL, Hooper LV. Epithelial antimicrobial defence of the skin and intestine. *Nat Rev Immunol* 2012;12:503–516.
- Lehotzky RE, Partch CL, Mukherjee S, Cash HL, Goldman WE, Gardner KH, Hooper LV. Molecular basis for peptidoglycan recognition by a bactericidal lectin. *Proc Natl Acad Sci U S A* 2010;107:7722–7727.
- Ogawa H, Fukushima K, Naito H, Funayama Y, Unno M, Takahashi K, Kitayama T, Matsuno S, Ohtani H, Takasawa S, Okamoto H, Sasaki I. Increased expression of HIP/PAP and regenerating gene III in human inflammatory bowel disease and a murine bacterial reconstitution model. *Inflamm Bowel Dis* 2003;9:162–170.
- Cayrol C, Girard JP. IL33: an alarmin cytokine with crucial roles in innate immunity, inflammation and allergy. *Curr Opin Immunol* 2014;31:31–37.
- Pichery M, Mirey E, Mercier P, Lefrancais E, Dujardin A, Ortega N, Girard JP. Endogenous IL33 is highly expressed in mouse epithelial barrier tissues, lymphoid organs, brain, embryos, and inflamed tissues: in situ analysis using a novel Il-33-LacZ gene trap reporter strain. *J Immunol* 2012;188:3488–3495.
- Duan L, Chen J, Zhang H, Yang H, Zhu P, Xiong A, Xia Q, Zheng F, Tan Z, Gong F, Fang M. Interleukin-33 ameliorates experimental colitis through promoting Th2/Foxp3(+) regulatory T-cell responses in mice. *Mol Med* 2012;18:753–761.
- Kurowska-Stolarska M, Kewin P, Murphy G, Russo RC, Stolarski B, Garcia CC, Komai-Koma M, Pitman N, Li Y, Niedbala W, McKenzie AN, Teixeira MM, Liew FY, Xu D. IL33 induces antigen-specific IL5+ T cells and promotes allergic-induced airway inflammation independent of IL4. *J Immunol* 2008;181:4780–4790.
- Oboki K, Ohno T, Kajiwara N, Arae K, Morita H, Ishii A, Nambu A, Abe T, Kiyonari H, Matsumoto K, Sudo K, Okumura K, Saito H, Nakae S. IL33 is a crucial amplifier of innate rather than acquired immunity. *Proc Natl Acad Sci U S A* 2010;107:18581–18586.
- Sedhom MA, Pichery M, Murdoch JR, Foligné B, Ortega N, Normand S, Mertz K, Sanmugalingam D, Brault L, Grandjean T, Lefrancais E, Fallon PG, Quesniaux V, Peyrin-Biroulet L, Cathomas G, Junt T, Chamaillard M, Girard JP, Ryffel B. Neutralisation of the interleukin-33/ST2 pathway ameliorates experimental colitis through enhancement of mucosal healing in mice. *Gut* 2013;62:1714–1723.
- Smithgall MD, Comeau MR, Yoon BR, Kaufman D, Armitage R, Smith DE. IL33 amplifies both Th1- and Th2-type responses through its activity on human basophils, allergen-reactive Th2 cells, iNKT and NK cells. *Int Immunol* 2008;20:1019–1030.
- Waddell A, Vallance JE, Moore PD, Hummel AT, Wu D, Shanmukhappa SK, Fei L, Washington MK, Minar P, Coburn LA, Nakae S, Wilson KT, Denson LA, Hogan SP, Rosen MJ. IL33 signaling protects from murine oxazolone colitis by supporting intestinal epithelial function. *Inflamm Bowel Dis* 2015;21:2737–2746.
- Moussion C, Ortega N, Girard JP. The IL1-like cytokine IL33 is constitutively expressed in the nucleus of endothelial cells and epithelial cells in vivo: a novel 'alarmin'? *PLoS One* 2008;3:e3331.
- Whitehead RH, Robinson PS. Establishment of conditionally immortalized epithelial cell lines from the intestinal tissue of adult normal and transgenic mice. *Am J Physiol Gastrointest Liver Physiol* 2009;296:G455–G460.
- Cua DJ, Tato CM. Innate IL17-producing cells: the sentinels of the immune system. *Nat Rev Immunol* 2010;10:479–489.
- Choi SM, McAleer JP, Zheng M, Pociask DA, Kaplan MH, Qin S, Reinhart TA, Kolls JK. Innate Stat3-mediated induction of the antimicrobial protein Reg3gamma is required for host defense against MRSA pneumonia. *J Exp Med* 2013;210:551–561.
- Lee KS, Kalantzis A, Jackson CB, O'Connor L, Murata-Kamiya N, Hatakeyama M, Judd LM, Giraud AS, Menheniott TR. *Helicobacter pylori* CagA triggers expression of the bactericidal lectin REG3gamma via gastric STAT3 activation. *PLoS One* 2012;7:e30786.
- Chen H, Yang Z, Ding C, Chu L, Zhang Y, Terry K, Liu H, Shen Q, Zhou J. Discovery of O-alkylamino tethered niclosamide derivatives as potent and orally bioavailable anticancer agents. *ACS Med Chem Lett* 2013;4:180–185.
- Gough DJ, Koetz L, Levy DE. The MEK-ERK pathway is necessary for serine phosphorylation of mitochondrial STAT3 and Ras-mediated transformation. *PLoS One* 2013;8:e83395.
- Yokogami K, Wakisaka S, Avruch J, Reeves SA. Serine phosphorylation and maximal activation of STAT3 during CNTF signaling is mediated by the rapamycin target mTOR. *Curr Biol* 2000;10:47–50.
- Seki K, Sanada S, Kudinova AY, Steinhauser ML, Handa V, Gannon J, Lee RT. Interleukin-33 prevents apoptosis and improves survival after experimental myocardial infarction through ST2 signaling. *Circ Heart Fail* 2009;2:684–691.
- Zhang L, Lu R, Zhao G, Pflugfelder SC, Li DQ. TLR-mediated induction of pro-allergic cytokine IL33 in ocular mucosal epithelium. *Int J Biochem Cell Biol* 2011;43:1383–1391.
- Mori N, Yamada Y, Ikeda S, Yamasaki Y, Tsukasaki K, Tanaka Y, Tomonaga M, Yamamoto N, Fujii M. Bay 11-7082 inhibits transcription factor NF-kappaB and induces apoptosis of HTLV-I-infected T-cell lines and primary adult T-cell leukemia cells. *Blood* 2002;100:1828–1834.
- Suzuki A, Hanada T, Mitsuyama K, Yoshida T, Kamizono S, Hoshino T, Kubo M, Yamashita A, Okabe M, Takeda K, Akira S, Matsumoto S, Toyonaga A, Sata M, Yoshimura A. CIS3/SOCS3/SSI3 plays a negative regulatory role in STAT3 activation and intestinal inflammation. *J Exp Med* 2001;193:471–481.

27. Yang EJ, Lee J, Lee SY, Kim EK, Moon YM, Jung YO, Park SH, Cho ML. EGCG attenuates autoimmune arthritis by inhibition of STAT3 and HIF-1alpha with Th17/Treg control. *PLoS One* 2014;9:e86062.
28. Matta BM, Lott JM, Mathews LR, Liu Q, Rosborough BR, Blazar BR, Turnquist HR. IL33 is an unconventional Alarmin that stimulates IL2 secretion by dendritic cells to selectively expand IL33R/ST2+ regulatory T cells. *J Immunol* 2014;193:4010–4020.
29. Mangan PR, Harrington LE, O'Quinn DB, Helms WS, Bullard DC, Elson CO, Hatton RD, Wahl SM, Schoeb TR, Weaver CT. Transforming growth factor-beta induces development of the T(H)17 lineage. *Nature* 2006;441:231–234.
30. Lopetuso LR, Scaldaferrri F, Pizarro TT. Emerging role of the interleukin (IL)-33/ST2 axis in gut mucosal wound healing and fibrosis. *Fibrogenesis Tissue Repair* 2012;5:18.
31. Pastorelli L, Garg RR, Hoang SB, Spina L, Mattioli B, Scarpa M, Fiocchi C, Vecchi M, Pizarro TT. Epithelial-derived IL33 and its receptor ST2 are dysregulated in ulcerative colitis and in experimental Th1/Th2 driven enteritis. *Proc Natl Acad Sci U S A* 2010;107:8017–8022.
32. Milovanovic M, Volarevic V, Radosavljevic G, Jovanovic I, Pejnovic N, Arsenijevic N, Lukic ML. IL33/ST2 axis in inflammation and immunopathology. *Immunol Res* 2012;52:89–99.
33. Hancock RE, Haney EF, Gill EE. The immunology of host defense peptides: beyond antimicrobial activity. *Nat Rev Immunol* 2016;16:321–334.
34. Malik A, Sharma D, Zhu Q, Karki R, Guy CS, Vogel P, Kanneganti TD. IL33 regulates the IgA-microbiota axis to restrain IL1alpha-dependent colitis and tumorigenesis. *J Clin Invest* 2016;126:4469–4481.
35. Schiering C, Krausgruber T, Chomka A, Fröhlich A, Adelman K, Wohlfert EA, Pott J, Griseri T, Bollrath J, Hegazy AN, Harrison OJ, Owens BMJ, Löhning M, Belkaid Y, Fallon PG, Powrie F. The alarmin IL33 promotes regulatory T-cell function in the intestine. *Nature* 2014;513:564–568.
36. Seidelin JB, Coskun M, Kvist PH, Holm TL, Holgersen K, Nielsen OH. IL33 promotes GATA-3 polarization of gut-derived T cells in experimental and ulcerative colitis. *J Gastroenterol* 2015;50:180–190.
37. Loonen LM, Stolte EH, Jaklofsky MT, Meijerink M, Dekker J, van Baaren P, Wells JM. REG3gamma-deficient mice have altered mucus distribution and increased mucosal inflammatory responses to the microbiota and enteric pathogens in the ileum. *Mucosal Immunol* 2014;7:939–947.
38. Qin H, Wang L, Feng T, Elson CO, Niyongere SA, Lee SJ, Reynolds SL, Weaver CT, Roarty K, Serra R, Benveniste EN, Cong Y. TGF-beta promotes Th17 cell development through inhibition of SOCS3. *J Immunol* 2009;183:97–105.
39. Muller CA, Autenrieth IB, Peschel A. Innate defenses of the intestinal epithelial barrier. *Cell Mol Life Sci* 2005;62:1297–1307.
40. Lee J, Jung E, Kim YS, Park D, Toyama K, Date A, Lee J. Phloridzin isolated from *Acanthopanax senticosus* promotes proliferation of alpha6 integrin (CD 49f) and beta1 integrin (CD29) enriched for a primary keratinocyte population through the ERK-mediated mTOR pathway. *Arch Dermatol Res* 2013;305:747–754.
41. Yang YH, Chen K, Li B, Chen JW, Zheng XF, Wang YR, Jiang SD, Jiang LS. Estradiol inhibits osteoblast apoptosis via promotion of autophagy through the ER-ERK-mTOR pathway. *Apoptosis* 2013;18:1363–1375.
42. Zhou J, Wulfkühle J, Zhang H, Gu P, Yang Y, Deng J, Margolick JB, Liotta LA, Petricoin E 3rd, Zhang Y. Activation of the PTEN/mTOR/STAT3 pathway in breast cancer stem-like cells is required for viability and maintenance. *Proc Natl Acad Sci U S A* 2007;104:16158–16163.
43. Chung J, Uchida E, Grammer TC, Blenis J. STAT3 serine phosphorylation by ERK-dependent and -independent pathways negatively modulates its tyrosine phosphorylation. *Mol Cell Biol* 1997;17:6508–6516.
44. Sanjana NE, Shalem O, Zhang F. Improved vectors and genome-wide libraries for CRISPR screening. *Nat Methods* 2014;11:783–784.
45. Klindworth A, Pruesse E, Schweer T, Peplies J, Quast C, Horn M, Glöckner FO. Evaluation of general 16S ribosomal RNA gene PCR primers for classical and next-generation sequencing-based diversity studies. *Nucleic Acids Res* 2013;41:e1.
46. Quast C, Pruesse E, Yilmaz P, Gerken J, Schweer T, Yarza P, Peplies J, Glöckner FO. The SILVA ribosomal RNA gene database project: improved data processing and web-based tools. *Nucleic Acids Res* 2013;41:D590–D596.

Received October 4, 2017. Accepted February 20, 2019.

Correspondence

Address correspondence to: Yingzi Cong, PhD, Department of Microbiology and Immunology, University of Texas Medical Branch, 4.142C Medical Research Building, 301 University Boulevard, Galveston, Texas 77555-1019. e-mail: yicong@utmb.edu; fax: (409) 772-5065; or Daiwen Chen, PhD, Key Laboratory of Animal Disease-Resistance Nutrition, Animal Nutrition Institute, Sichuan Agricultural University, Yaan, Sichuan, China, 625014. e-mail: dwchen@sicau.edu.cn; fax: 86-28-82652669.

Acknowledgements

The authors thank Dr. Linsey Yeager of The University of Texas Medical Branch for proofreading the manuscript. All authors had access to the study data and had reviewed and approved the final manuscript. Conceptualization: Yi Xiao, Daiwen Chen, and Yingzi Cong. Methodology: Yi Xiao, Xiangsheng Huang, Sara M. Dann, Daiwen Chen, and Yingzi Cong. Investigation: Yi Xiao, Xiangsheng Huang, Ye Zhao, Feidi Chen, Mingming Sun, Wenjing Yang, Liang Chen, Suxia Yao, Alex Peniche, Sara M. Dann, George Golovko, Daiwen Chen, and Yingzi Cong. Resources: Jiaren Sun, Yuriy Fofanov, Yinglei Miao, and Zhanju Liu. Writing and original draft preparation: Yi Xiao and Yingzi Cong. Writing and review and editing: Yi Xiao, Sara M. Dann, Daiwen Chen, and Yingzi Cong with input from all other authors. Supervision: Daiwen Chen and Yingzi Cong; Funding acquisition: Yingzi Cong.

Conflicts of interest

The authors disclose no conflicts.

Funding

This work was supported by National Institutes of Health grants DK098370, DK105585, and DK112436; John Sealy Memorial Endowment Fund (Y.C.); and China Scholarship Council (Y.X.) fellowship.